Independent Component and Source Information Flow Analysis of Default-Mode EEG in Autism

Robert J. Gougelet
Department of Cognitive Science
University of California - San Diego
La Jolla, CA 92093
rgougele@ucsd.edu

Abstract

Idling signatures of the resting brain have become a recent topic of interest in the functional MRI literature, wherein baseline activation signals are spatially localized and interpreted as a connected and synchronized neural network, instantiating a so-called default mode network (DMN). Further work is being done to couple MRI and EEG functional and structural connectivity analyses of this network. In contrast, little work has been done to examine the effective EEG connectivity of the DMN using causal information flow techniques, particularly in autism. The goal of this paper is to examine baseline EEG data of individuals with autism compared to non-autistic individuals to identify properties and changes of causal information flow among maximally independent components of the EEG signal in a default state. The qualitative analysis within this paper suggests greater information flow and activity during rest especially among local components in autism, although quantitative analyses are necessary and important. Future comparisons of functional and diffusion MRI data of the same subjects will provide a multimodal approach to extracting distinct features of the DMN across populations, in order to identify robust functional, structural, and effective, connectivity characterizations of neural deficits in autism.

1 Introduction

The DMN has been identified as the areas of the brain that are active during visual fixation and eyes-closed rest conditions [20]. These areas are identified by subtracting task state data from control state data, i.e. reverse subtraction, as opposed to subtracting control state data from task state data, the method currently dominating fMRI literature [21]. These negative activations seem to reflect an idling or default state of the brain, and occur independent of the subtracted positive task. The medial prefrontal cortex (mPFC), posterior cingulate cortex (PCC), the medial posterior cortex (mPC), lateral posterior cortex (lPC), and inferior posterior cortex (iPC), have been identified as the DMN regions of interest [17, 20, 21]. Interestingly the DMN has been implicated in a variety of task-negative resting states, implicating particular subsystems of the DMN, including a(n): dorsal attention network, visual processing network, auditory-phonological network, sensorimotor network, and a self-referential network [17]. Within the past decade, these findings have drawn much attention and interest to the characterization of the DMN in control and disease populations.

The DMN provides a complementary explanatory mechanism to account for deficits in a variety of mental disorders, alongside the more studied discrepant features of task-positive network deficits in mental disorders. As such, aberrant DMN activity in Alzheimer's, schizophrenia, depression, anxiety, epilepsy, attention deficit/hyperactivity, and autism spectrum disorders (ASD) has been uncovered since the network's first discovery [3]. Interestingly, the self-referential areas of the DMN seem to activate to a greater degree in depression, when self-referential thought and rumination run

rampant [7]. Considering the obsessive self-regulatory and self/other-referential symptoms of ASD, dysfunction in the DMN might provide the missing causal link among the spectrum of deficits seen in ASD.

Unfortunately, little work exists examining the DMN in autism [3], despite abundant research in task-positive conditions. With fMRI, Kennedy et al. [12] showed that adult autistics failed to deactivate their DMN's during three versions of an emotional Stroop task. Kennedy and Courchesne [11] showed reduced functional MRI connectivity in DMN but not in task-positive networks, again in adult autistics. Cherkassky et al. [5] observed no difference in DMN activation during rest in autistic adults vs. control, but observed decreased connectivity across anterior and posterior cingulate cortex, the area implicated by Mantini et al. [17] to be involved in self-referential thought. Further, it has been suggested that joint dysfunction of the mirror neuron system, responsible for imitation and presumably self-other differentiation, and the DMN could lead to the deficits in self-other processing seen in autism [8]. Though spatially informative, these fMRI studies only discuss correlation of activity among these brain regions, and do less to characterize the causal dynamics of the DMN in the default state, particularly in a time-sensitive manner. Further, the findings are fairly inconclusive and warrant more investigation.

With the scant fMRI research of the DMN in autism, there is even less research using EEG measures of DMN connectivity [4] and, to this date, none examining independent EEG components (discussed later in this paper) DMN connectivity in autism. Chen et al. [4] did identify the spectral distribution of EEG field powers across channels on the scalp during rest, indicating delta, beta-2, gamma activity in anterior regions, alpha-1, alpha-2, beta-1 activity in posterior regions, and theta activity in anterior-posterior regions. Due to electrical volume conductance, these measures may not reflect the actual activation of the neural populations generating the EEG signal. Further, these findings are from a healthy adult population. Still, with these findings we might expect to find in ASD an increased activation of these frequencies in these areas, or less connectivity among these areas within these frequencies.

Using a graph theoretic approach, Barttfeld et al. [1] found distinct ASD EEG connectivity patterns within the delta range during rest. ASD subjects lacked long-range connections, with most prominent deficits in fronto-occipital connections, and increased short-range connections in lateral-frontal connections. Again, these findings are subject to problems with volume conductance. Indeed, Vissers et al. [22] suggest that this view of connectivity in ASD needs refinement, and that it fails to capture the different and complex patterns of connectivity in ASD. The goal of this paper is to provide a novel approach to understanding DMN connectivity in ASD, using source information flow analysis of maximally independent components in resting EEG data from individuals with ASD and controls.

2 Source Information Flow

2.1 Connectivity

There are three types of connectivity examined in the neuroscience literature: anatomical, functional, and effective connectivity [6]. Anatomical connectivity is concerned with using neurophysiology techniques like axon labeling or imaging techniques like diffusion weighted/tensor imaging to identify the existence of physiological connectivity among brain areas. These techniques are either invasive or fail to show the direction of connectivity. Functional connectivity generally concerns the correlation of fMRI activations of brain regions during tasks. Again, the directionality of excitatory or inhibitory action is not inferable, nor can the causal influence of one brain region on the other be identified. Effective connectivity, on the other hand, provides such causal directionality information and can be examined using Granger causality, or graph theoretic analyses. Graphs are generally not used in a directional manner in the literature, but when they are, they still only provide a descriptive account of network connectivity, and provide few statistically robust measures. Granger Causality techniques are more robust and are discussed in further detail below.

2.2 Granger Causality

2.2.1 Multivariate Autoregressive Modeling

Granger Causality involves a basic a priori assumption of stationarity of time-series data. With this assumption, one can generate a multivariate autoregressive model fit to multidimensional time-series data, including EEG data [18, 19]. Let $X := [x_1 ... x_T]$, where $x_t = [x_{1t} ... x_{Mt}]'$, be our M-dimensional time-series EEG data of time length T. Our autoregressive model VAR[p] is thus:

$$x_t = v + \sum_{k=1}^{p} A_k x_{t-k} + u_t$$

where p is the order of our model, x_t is our data at time t, v is an intercept that is, in practice, mean-subtracted out. The white noise process u_t, with zero-mean after mean-subtraction has the covariance matrix:

$$\Sigma = \langle u_t u_t^T \rangle$$

By using an adaptive window analysis that segments the data into windows and smooths the calculation of A_k over the windows across small time steps, we can induce a local stationarity and examine the changes in causal flow of non-stationary, i.e. dynamic EEG, data across time [17, 18]. Further, we can generate what is known as the direct Directed Transfer Function (dDTF) to conduct a frequency analysis of causality, identifying information flow with respect to particular frequencies.

2.2.2 Frequency measure of Granger Causality

Below we generate the Short-time direct Directed Transfer Function (SdDTF), as cited in [18,19] from [9, 10, 13, 14]. Assuming a process mean of zero, we have:

$$x_t = \sum_{k=1}^{p} A_k x_{t-k} + u_t \Rightarrow$$

$$u_t = \sum_{k=0}^{p} \hat{A}_k x_{t-k}, \text{ where } \hat{A}_k = -A_k \text{ and } \hat{A}_0 = -I$$

Applying the Fourier Transform, and taking a Z-transformation, we have:

$$U(f) = A(f)X(f), \text{ where } A(f) = \sum_{k=0}^{p} \hat{A}_k e^{-i2\pi fk}$$

We define the $(M \times M)$ spectral density matrix $S(f)$ and the transfer matrix $H(f) = A(f)^{-1}$ of the process $X(f)$ as:

$$S(f) := X(f)X(f)^* = H(f)\Sigma H(f)^{-1}$$

Therefore,

$$X(f) = A(f)^{-1}U(f) = H(f)U(f)$$

We also identify the partial coherence P_{ij} between channels i and j:

$$P_{ij}(f) := \frac{\hat{S}_{ij}(f)}{\sqrt{\hat{S}_{ii}(f)\hat{S}_{jj}(f)}}, \text{ and } \hat{S} = S^{-1}$$

From these, we define the squared Short-time direct Directed Transfer Function (SdDTF) from channel j to i, δ_{ij}:

$$\delta_{ij}^2(f,t) = \frac{|H_{ij}(f,t)|^2 |P_{ij}(f,t)|^2}{\Sigma_{f\tau}\Sigma_{m=1}^{M} |H_{mk}(f,\tau)|^2 |P_{mk}(f,\tau)|^2}$$

This function provides us with a measure of information flow, or conditional Granger Causality, from channel j to i within a window centered at time t with width τ at frequency f.

2.3 Independent Component Analysis

Independent component analysis (ICA) can be applied to time-series data to identify maximally independent components mixed within the signal [2, 14, 16] . In other words, finding a matrix, $\mathbf{W}$ and a vector, w, such that the elements of $\mathbf{u} = [u_1...u_N]'$ are statistically independent, given the linear transform $\mathbf{u} = \mathbf{W}\mathbf{x} + w$ of the random vector, $\mathbf{x} = [x_1...x_N]'$. This involves minimizing the mutual information I among the u_i: $I(u_i, u_j) = 0, \forall ij$, which depends on all higher-order statistics of u_i.

If we assume that the cumulative density function, $F_u(u)$, of each u_i has the same form after scaling and shifting, then we can maximize the entropy, $H(\mathbf{y})$, of the non-linearly transformed vector $\mathbf{y} = F_u(\mathbf{u})$, in a stochastic gradient descent manner on $\mathbf{W}$ and w:

$$\Delta\mathbf{W} \propto [\mathbf{W}']^{-1} + \hat{\mathbf{y}}\mathbf{x}', \Delta w \propto \hat{\mathbf{y}}$$

Where $\hat{\mathbf{y}} = [\hat{y_1}...\hat{y_N}]'$ and if $\mathbf{y} = F_u(\mathbf{u})$:

$$\hat{y_i} = \frac{\partial}{\partial y_i}\frac{\partial y_i}{\partial u_i} = \frac{\partial f_u(u_i)}{\partial F_u(u_i)}$$

An extension of the above algorithm involves determining whether the components u_i are subgaussian or supergaussian and adapting the stochastic gradient step appropriately [15]. After identification, the independent components of ICA can act as the time-series input to our source information flow analysis, conducted below.

3 Methods

The data were collected using a 21-channel EEG device at a sampling rate of 500Hz. Subjects were tasked with an eyes-closed resting and eyes-open fixation condition for five minutes. Data were collected pre- and post-treatment using a neurofeedback paradigm not discussed in this paper. Also collected in this study were fMRI and DTI data, along with anatomical scans, also not addressed in this paper. Data were cleaned and analyzed using EEGLAB and the Source Information Flow Toolbox (SIFT), a currently separate plug-in toolbox for EEGLAB [18].

ICA was run on the raw data, which included mastoid and vertical oculogram channels, and components containing eye or muscle artifacts were removed by eye. The remaining components were filtered from 2-40Hz using a causal filter supplied by SIFT. The remaining components were divided into five second epochs, and epochs were automatically and manually rejected containing noise not removed by filtering or ICA. The remaining epochs were fed into SIFT, wherein the dDTF was computed. The data were detrended and normalized according to the SIFT manual. A model order of 14 was used across both subjects, with a window size of 1 second and a step size of 0.01 seconds. Unfortunately, no stability and stationarity checks were applied. A time-frequency information flow plot was then produced; the current version of SIFT does not provide means to collapse across the time domain, so only the frequency information flow across components is relevant, and the time activations are superfluous.

4 Results and Discussion

The results of the source information flow analysis of components derived from an ASD subject in an eyes-closed condition are found in Figure 1. We see a large peak of alpha activity from component five to component one, six, and 12, and 14. These components seem to indicate strong local connectivity, considering their spatial similarity. The same can be said for component two, which has broad band interactions with components three, four, and 6. Similarly, component 10 has some broad band interaction with components seven and eight, also spatially similar components. Finally, component 13 has high alpha, perhaps Mu, directed interaction to components one, nine, 10, 12, and 14. In Figure 2, we see a closer look at component five, indicating the strongest interaction with component six. Overall, these findings suggest strong activation within a default-mode state,

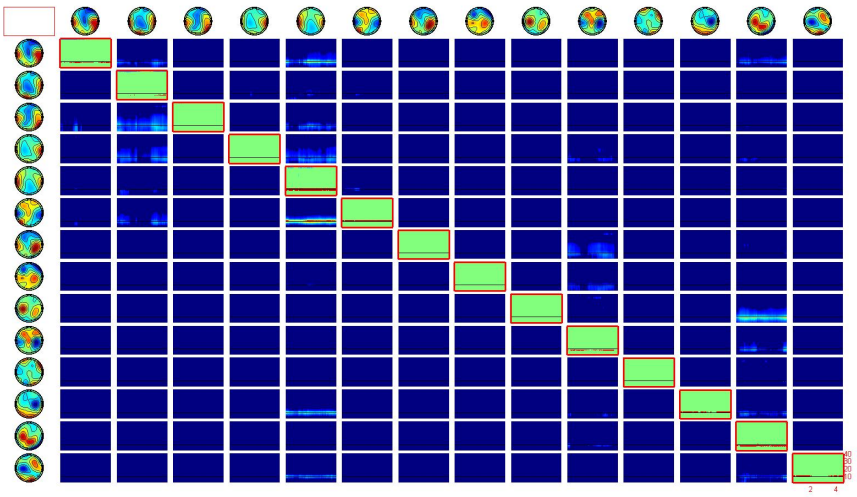

Figure 1: Source information flow from columns to rows as indicated by the dDTF in the off-diagonals. The topoplots along the top and left are the spatial locations of the components. Causal information flow is indicated by brightness from blue to red.

especially among local components. This is consistent with findings from other studies examining connectivity [1, 22].

The results of the source information flow analysis of components derived from a control subject in an eyes-closed condition are found in Figure 3. Component two shows slight directed information flow to component four, whereas component four shows information flow to components one and two, particularly in the low frequency ranges, normally attributed to long-range cortico-cortico [22] connections. Figure 4 provides a closer look of information flow between components two and four. Again, these findings suggest local connectivity is more apparent, but the extent of activation is much lower compared to the ASD subject. Both components five and seven seem to flow into component six with greater broad band activity, and these components seem less localized. Interestingly, component six seems to feed into component seven, suggesting mutual information flow. This interaction is further illustrated in Figure 5. Overall, the control subject demonstrates much less causal information flow compared to the ASD subject, again consistent with findings from the literature [1, 22].

At this time, interpretation of these results are qualitative and speculative. More subjects and statistical analyses will need to be included to provide definitive results. Future developments of this study would involve the use of better noise removal techniques. Inclusion of the eyes-closed condition would also provide further insights, especially comparing differences across conditions. Developing means to better identify spatial regions of interest is in order, so as to focus on predetermined areas involved in DMN processing. Mantini et al. [17] did identify characteristic EEG frequency band power configurations for the various sub-networks of the DMN, but did not look at ASD subjects and only worked in channel-space, but their findings could prove useful in categorizing components by spatial and frequency distributions. Incorporation of the available MRI data of these subjects would provide an anatomical and functional connectivity approach, allowing the complete connectivity analysis of these data. Further, comparison across pre- and post-treatment of the neurofeedback paradigm would shed light onto its efficacy in changing neural dynamics in autism.

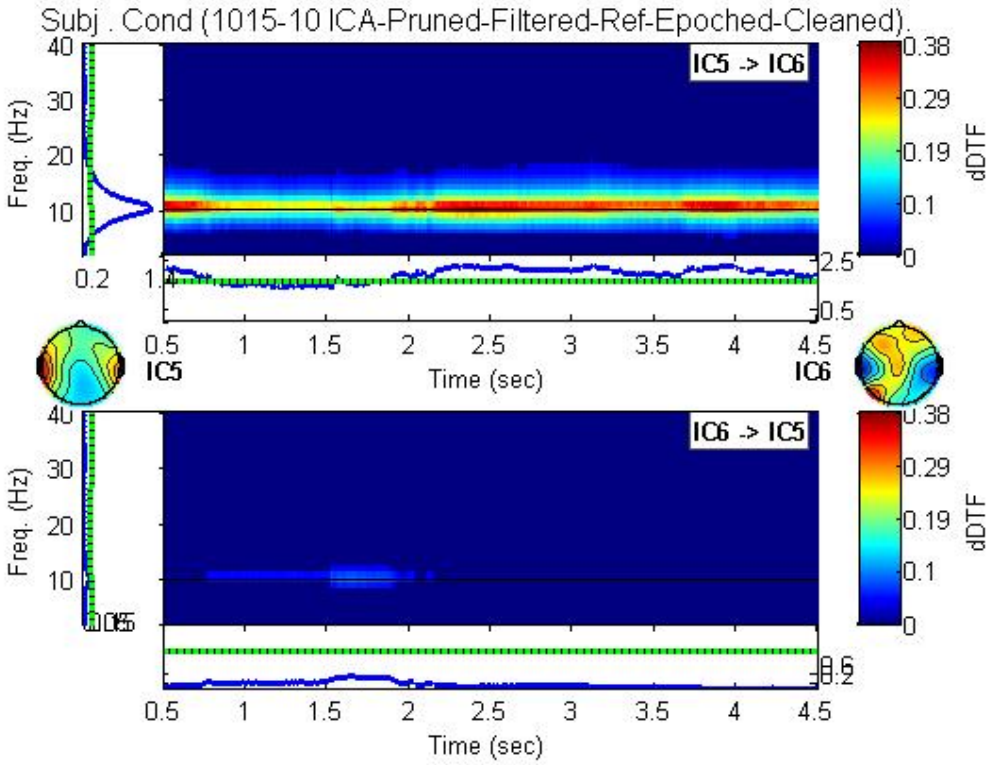

Figure 2: Time-frequency source information flow as indicated by the dDTF. Changes in frequency over time is superfluous in this image, and should be conceived of as an average. The topoplots on the left and right indicate the spatial locations of the components.

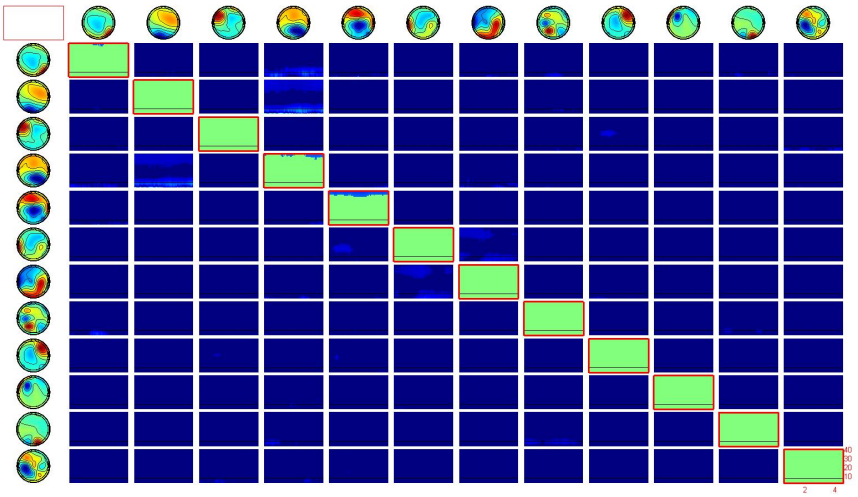

Figure 3: Source information flow from columns to rows as indicated by the dDTF in the off-diagonals. The topoplots along the top and left are the spatial locations of the components. Causal information flow is indicated by brightness from blue to red.

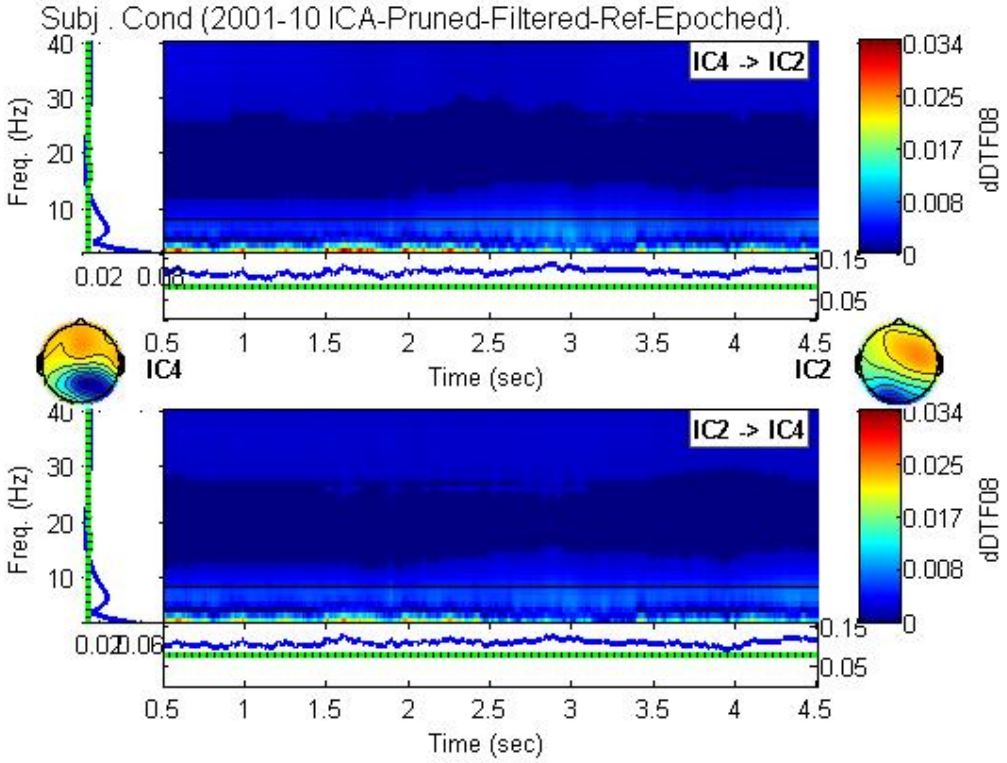

Figure 4: Time-frequency source information flow as indicated by the dDTF. Changes in frequency over time is superfluous in this image, and should be conceived of as an average. The topoplots on the left and right indicate the spatial locations of the components.

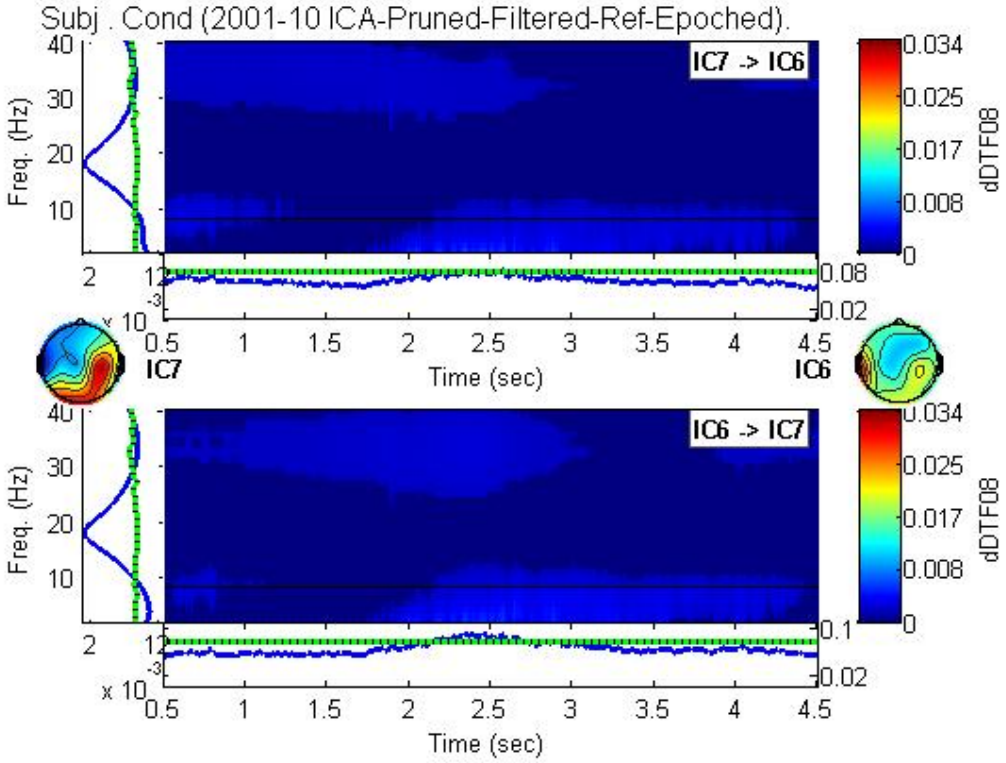

Figure 5: Time-frequency source information flow as indicated by the dDTF. Changes in frequency over time is superfluous in this image, and should be conceived of as an average. The topoplots on the left and right indicate the spatial locations of the components.

Acknowledgments

Thanks to Dr. Jaime Pineda for the data and Tim Mullen for discussion on the use of SIFT.

References

[1] Barttfeld, P., Wicker, B., Cukier, S., Navarta, S., Lew, S., & Sigman, M. (2011). A big-world network in ASD: Dynamical connectivity analysis reflects a deficit in long-range connections and an excess of short-range connections. Neuropsychologia, 49, 254-263.

[2] Bell, A. & Sejnowski, T. (1995). An information-maximization approach to blind separation and blind deconvolution. Neural Computation, 7(6), 1129-1159.

[3] Broyd, S. J., Demanuele, C., Debener, S., Helps, S. K., James, C. J., & Sonuga-Barke, E. J. S. (2009). Default-mode brain dysfunction in mental disorders: A systematic review. Neuroscience and Biobehavioral Reviews, 33, 279-296.

[4] Chen, A. C. N., Feng, W., Zhao, H., Yin, Y., & Wang, P. (2008). EEG default mode network in the human brain: Spectral regional field powers. NeuroImage, 41, 561-574.

[5] Cherkassky, V. L., Kana, R. K., Keller, T. A., & Just, M.A. (2006). Functional connectivity in baseline resting-state network in autism. NeuroReport, 17, 1687-1690.

[6] Friston, K. J. (1994). Functional and effective connectivity in neuroimaging: A synthesis. Human Brain Mapping, 2, 56-78.

[7] Greicius, M. D., Flores, B. H., Menon, V., Glover, G. H., Solvason, H. B., Kenna, H., Reiss, A. L., & Schatzberg, A. F. (2007) Resting-state functional connectivity in Major Depression: Abnormally increased contributions from subgenual cingulate cortex and thalamus. Biological Psychiatry, 62, 429-437.

[8] Iacoboni, M. (2006). Failure to deactivate in autism: The co-constitution of self and other. Trends in Cognitive Science, 10, 431-433.

[9] Kaminski, M., & Blinowska, K. J. (1991). A new method of the description of the information flow in brain structures. Biological Cybernetics, 65, 203-210.

[10] Kaminski, M., Ding, M., Truccolo, W., & Bressler, S. (2001). Evaluating causal relations in neural systems: Granger causality, directed transfer function and statistical assessment of significance. Biological Cybernetics, 85, 145-157.

[11] Kennedy, D. P., & Courchesne, E. (2008). The intrinsic functional organization of the brain is altered in autism. NeuroImage, 39, 1877-1885.

[12] Kennedy, D. P., Redcay, E., & Courchesne, E. (2006). Failing to deactivate: Resting functional abnormalities in autism. Proceedings of the National Academies of Sciences of the USA, 103, 8275-8280.

[13] Korzeniewska, A. (2003). Determination of information flow direction among brain structures by a modified directed transfer function (dDTF) method. Journal of Neuroscience Methods, 125, 195-207.

[14] Korzeniewska, A., Crainiceanu, M., Kus, R., Franaszczuk, P., & Crone, N. (2008). Dynamics of event-related causality in brain electrical activity. Human Brain Mapping, 29, 1170-1192.

[15] Lee, T. W., Girolami, M., & Sejnowski, T. J. (1999). Independent component analysis using an extended infomax algorithm for mixed subgaussian and supergaussian sources. Neural computation, 11(2), 417-441.

[16] Makeig, S., Bell, A. J., Jung, T., Sejnowski, T. J. (1996). Independent component analysis of electroencephalographic data. Advances in Neural Information Processing Systems, 8, 145-151.

[17] Mantini, D., Perrucci, M. G., Gratta, C. D., Romani, G. L., Corbetta, M. (2007). Electrophysiological signatures of resting state networks in the human brain. Proceedings from the National Academies of Sciences of the USA, 104(32), 13170-13175

[18] Mullen, T., Delorme, A., Kothe, C., & Makeig, S. (2010). An Electrophysiological Information Flow Toolbox for EEGLAB. Proceedings from Society for Neuroscience. San Diego, CA.

[19] Mullen, T. (2010). Analysis of neuronal source dynamic during seizure using vector autoregressive models, ICA, Sparse Bayesian Learning and ECoG (Unpublished academic paper). University of California - San Diego, San Diego, CA.

[20] Raichle, M. E., MacLeod, A. M, Snyder, A. Z., Powers, W. J., Gusnard, D. A., & Shulman, G. L. (2001). A default mode of brain function. Proceedings of the National Academies of Sciences of the USA, 98, 676-682.

[21] Raichle, M.E., & Snyder, A. Z. (2007). A default mode of brain function: A brief history of an evolving idea. NeuroImage, 37, 1083-1090.

[22] Vissers, M. E., Cohen, M. X., & Geurts, H. M. (2012) Brain connectivity and high functioning autism: A promising path of research that needs refined models, methodological convergence, and stronger behavioral links. Neuroscience and Biobehavioral Reviews, 36, 604-625.